Inorganic Chemistry

Article

pubs.acs.org/IC

The Parent Li(OH)FeSe Phase of Lithium Iron Hydroxide Selenide Superconductors

Daniel N. Woodruff,[†] Francesca Schild,[†] Craig V. Topping,[‡] Simon J. Cassidy,[†] Jack N. Blandy,[†,§] Stephen J. Blundell,[‡] Amber L. Thompson,[†] and Simon J. Clarke*[,†]

[†]Department of Chemistry, University of Oxford, Inorganic Chemistry Laboratory, South Parks Road, Oxford, OX1 3QR, UK

[‡]Department of Physics, University of Oxford, Clarendon Laboratory, Parks Road, Oxford, OX1 3PU, UK

[§]Diamond Light Source Ltd., Harwell Science and Innovation Campus, Didcot, OX11 0DE, UK

Supporting Information

ABSTRACT: Lithiation of hydrothermally synthesized $Li_{1-x}Fe_x(OH)Fe_{1-y}Se$ turns on high-temperature superconductivity when iron ions are displaced from the hydroxide layers by reductive lithiation to fill the vacancies in the iron selenide layers. Further lithiation results in reductive iron extrusion from the hydroxide layers, which turns off superconductivity again as the stoichiometric composition Li(OH)FeSe is approached. The results demonstrate the twin requirements of stoichiometric FeSe layers and reduction of Fe below the +2 oxidation state as found in several iron selenide superconductors.

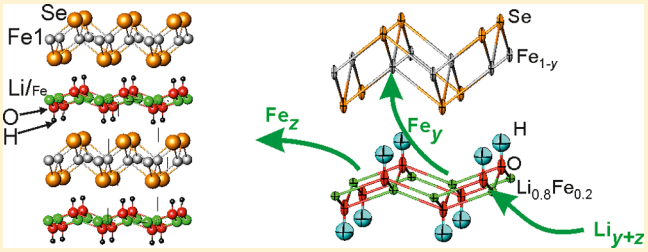

INTRODUCTION

Iron selenides have emerged as an important class of iron-based superconductor. $Fe_{1.01}Se$ is a superconductor with a transition temperature T_c of 8.5 K,[1] which is very sensitive to composition.[2] $K_{0.8}Fe_{1.6}Se_2$ and related phases[3] contain large concentrations of vacancies in the selenide layers,[4] which are detrimental to superconductivity, but regions of these samples may be vacancy-free and exhibit superconductivity.[5] Iron selenides in which the iron selenide layers contain few or no vacancies and in which iron is reduced below the +2 oxidation state show high-temperature superconductivity. Examples are alkali metal/ammonia intercalates of FeSe[6−8] and the recently discovered[9] hydroxide selenides $Li_{1-x}Fe_x(OH)Fe_{1-y}Se$, synthesized hydrothermally with $x \approx 0.2$ and $0.02 \leq y \leq 0.15$, which superconduct when $y < 0.05$.[10] We quantified the relationship between composition, structure, and superconducting T_c in these hydroxide selenides and have shown that reductive lithiation using Li in liquid ammonia (Li/NH_3), following the hydrothermal synthesis, reduces y to zero: incoming lithium displaces iron ions from the hydroxide layers into the vacant sites in the selenide layers (Figure 1) according to eq 1 yielding bulk superconducting compositions $Li_{1-x+y}Fe_{x-y}(OH)FeSe$.[10]

$$y\mathrm{Li} + \mathrm{Li}_{1-x}\mathrm{Fe}_x(\mathrm{OH})\mathrm{Fe}_{1-y}\mathrm{Se} \rightarrow \mathrm{Li}_{1-x+y}\mathrm{Fe}_{x-y}(\mathrm{OH})\mathrm{FeSe} \quad (1)$$

This report of the control of these compounds was in principle not able to disentangle the importance of reduction of Fe below the +2 oxidation state and full occupancy of the Fe sites in the selenide layer. Here we extend the soft chemistry of these compounds to approach the composition Li(OH)FeSe, which is not a superconductor, showing that reduction of iron below the +2 oxidation state is essential for superconductivity, in line with a recent computational report.[11]

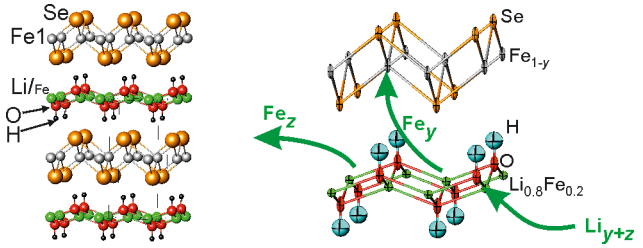

Figure 1. Structure of $Li_{1-x}Fe_x(OH)Fe_{1-y}Se$ and a schematic of the reactions described by eq 1 ($z = 0$) and eq 2 ($z > 0$) showing the displacement of iron by incoming Li.

Furthermore, some superconducting compositions synthesized hydrothermally show an apparent magnetic ordering transition at ~12 K, which has been ascribed to ferromagnetic ordering of the Fe^{2+} moments in the $Li_{0.8}Fe_{0.2}(OH)$ layers,[12] although other experiments initially suggested that these iron ions participate in anti-ferromagnetism.[13] In this article we also clarify this magnetism in the $Li_{0.8}Fe_{0.2}(OH)$ layers of hydrothermally synthesized samples that lie outside the superconducting regime.

Received: July 22, 2016
Published: September 22, 2016

DOI: 10.1021/acs.inorgchem.6b01734
Inorg. Chem. 2016, 55, 9886−9891

EXPERIMENTAL SECTION

Synthesis. Hydrothermal synthesis of $Li_{1-x}Fe_x(OH)Fe_{1-y}Se$ phases was performed using modifications of the methods reported in the literature.[9,10,12] We used presynthesized[2] $Fe_{1.01}Se$ as the source of Se and most of the Fe and excess LiOH to provide basic conditions. We exerted some control over the Fe/Se ratio in the products by including additional Fe powder in the synthesis. We also tested a route in which elemental Se and Fe were the sole sources of these elements. This enabled products to be synthesized hydrothermally with a larger Fe deficiency in the selenide layers of $Li_{1-x}Fe_x(OH)Fe_{1-y}Se$ (y as large as 0.2) than has been reported previously. However, the use of elemental reagents resulted in the persistence of poorly crystalline tetragonal FeSe as a minority phase. Further synthetic and characterization details are reported as Supporting Information (Tables S1 and S2; Figures S1–S4).

Subsequent lithiation of hydrothermally synthesized materials (Figure 1) proceeds according to eq 1.[10]

The reduced products are superconducting.[10] Reduction of iron goes hand-in-hand with the filling of the vacancies in the iron selenide layers, so it remains unclear whether both of these changes are essential for superconductivity. We address this question by demonstrating the different chemistry with three lithiation reagents: Li/NH_3, lithium naphthalenide (Li–Np) in tetrahydrofuran (THF), and n-butyl lithium (n-BuLi) in hexane. The lithiations were performed using standard Schlenk line techniques, taking into account potential hazards. In particular, ammonia is toxic and has a high vapor pressure, and the excess unreacted n-BuLi must be destroyed carefully after isolation of the solid products. The products were analyzed using in situ diffraction methods, ex situ diffraction methods, and magnetometry as described below. Full synthetic and characterization details and tables of results are included as Supporting Information (Tables S3 and S4 and Figures S9–S21).

Diffraction Measurements. Ex situ powder X-ray diffraction (PXRD) measurements (see Supporting Information) were performed at ambient temperature on the beamline I11 at the Diamond Light Source Ltd. Samples were ground with amorphous boron to limit X-ray absorption and minimize preferred orientation and were sealed inside 0.5 mm diameter borosilicate glass capillaries. Diffraction patterns were measured using Si-calibrated X-rays with approximate wavelength 0.82 Å using the multianalyzer crystal detector bank. Single-crystal diffraction measurements (see Supporting Information) were performed on small (~10 × 10 × 1 μm) crystals using the I19 diffractometer at Diamond using 0.69 Å X-rays. Powder neutron diffraction (PND) measurements were performed on the D2B instrument at the Institut Laue Langevin (ILL), Grenoble, France, in the temperature range from 5 K to room temperature using neutrons of wavelength 1.59 Å. Additional neutron diffraction measurements at room temperature were performed on the GEM or HRPD instruments at the ISIS Pulsed Neutron and Muon Source, U.K. Single-crystal diffraction data were analyzed using CRYSTALS,[14] and powder diffraction data were analyzed using TOPAS Academic.[15] In situ measurement of the lithiation reactions was performed on the I12 diffractometer at Diamond using the method previously described.[8] Further details are reported in the Supporting Information.

Magnetometry. Direct-current (DC) and alternating-current (AC) magnetometry was performed on powder samples using a Quantum Design MPMS-XL magnetometer. Samples were sequestered from air in gelatin capsules. DC volume magnetic susceptibilities χ were estimated as the sample magnetization (M) divided by the applied DC field (H) using the SI unit convention and are dimensionless. Measurements were made on warming after cooling in zero applied field (zero-field-cooled; ZFC) and after cooling in the measuring field (field-cooled; FC). The DC susceptibilities of the superconducting samples were corrected for the effect of demagnetizing fields arising from the shape of the sample.[16] AC susceptibilities approximated as M_{AC}/H_{AC} were measured in zero applied DC field with an AC drive amplitude of 4 mT and were reported as in-phase (χ') and out-of-phase (χ'') components. Drive frequencies ranged from 10 to 1000 Hz.

RESULTS

Comparison of Lithiating Agents. First we compared different lithiation reagents using a single hydrothermally synthesized, non-superconducting sample of refined composition $Li_{0.82(1)}Fe_{0.18(1)}(OH)Fe_{0.95(1)}Se$ (i.e., with a relatively low concentration of vacancies in the iron selenide layer), which displayed (Figure 2) the magnetic transition at 12 K discussed

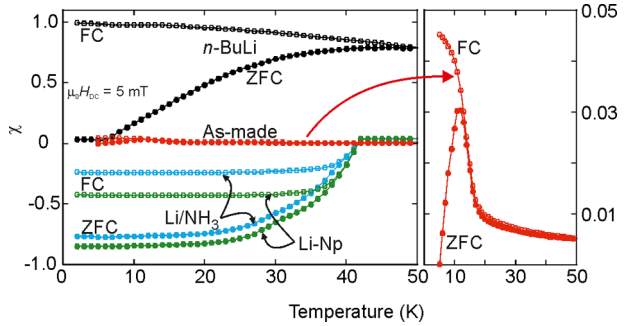

Figure 2. DC susceptibility measurements showing the turning on of superconductivity with the reaction of a single sample of $Li_{0.82(1)}Fe_{0.18(1)}(OH)Fe_{0.95(1)}Se$ (red) with Li/NH_3 (blue) and Li–Np (green) reagents; the absence of a superconducting transition and the formation of elemental iron when the lithiating agent is n-BuLi (black). The enlargement shows the magnetic transition.

further below. Structure refinements are presented in Table S3 and Figure S9; Figure 2 compares the magnetic susceptibilities of the products. The products with Li/NH_3 and Li–Np had very similar refined compositions and unit cell parameters ($a \approx$ 3.77 Å, $c \approx$ 9.35 Å). In both cases the c/a ratio increased by 1.9%, and the increase in the occupancy of the Fe site in the selenide layer (to 1.0) was matched by the increase of the lithium occupancy in the hydroxide layer; at the 3σ level there was no change in the refined total iron content. Both products were bulk superconductors with $T_c \approx$ 40 K, in line with our previous observations.[10] The magnetic transition at ~12 K was no longer evident. During the isolation of the products of these reactions it was evident, from the fact that the solutions had decolorized, that complete consumption of the solvated electron solution or the naphthalenide radical anion occurred in the course of the reactions even when an excess was used.

The use of n-BuLi provided a stark contrast and enabled new compositions to be accessed through further lithiation than seems possible using Li/NH_3[10] and Li–Np. The increase in the c lattice parameter to ~9.6 Å (Table S3) resulted in an increase in the c/a ratio of 5.1%, much larger than when Li–Np or Li/NH_3 solutions were used. Furthermore, the product had a greatly enhanced magnetic susceptibility consistent with the presence of 2.4% by mass of ferromagnetic elemental iron expelled according to eq 2, and there was no evidence for a superconducting transition superimposed on this background magnetism. It was also evident that excess n-BuLi was not decomposed by the suspended solid.

Structure refinement (Table S3 and Figure S9) showed that with n-BuLi, iron is again displaced into the selenide layer to fill the vacancies, but the Li content in the hydroxide layer increases by a larger amount: further Fe is expelled from the hydroxide layer as a separate elemental phase according to eq 2, extending the range of accessible phases:

DOI: 10.1021/acs.inorgchem.6b01734
Inorg. Chem. 2016, 55, 9886–9891

$$(y + z)\mathrm{Li} + \mathrm{Li}_{1-x}\mathrm{Fe}_x(\mathrm{OH})\mathrm{Fe}_{1-y}\mathrm{Se} = \mathrm{Li}_{1-x+y+z}\mathrm{Fe}_{x-y-z}(\mathrm{OH})\mathrm{FeSe} + z\mathrm{Fe} \quad (2)$$

where $0 \leq z \leq x-y$

In Situ Diffraction Measurements. The different reactivities using Li−Np and *n*-BuLi as lithiating reagents were probed by in situ PXRD measurements on a further two hydrothermally synthesized samples with different Fe contents (y = 0.05(1) and 0.14(1)) in the selenide layers (Table S4 and Figure S10). The contrast between the lithiation using Li−Np and *n*-BuLi for both cases is shown in Figure 3. With Li−Np

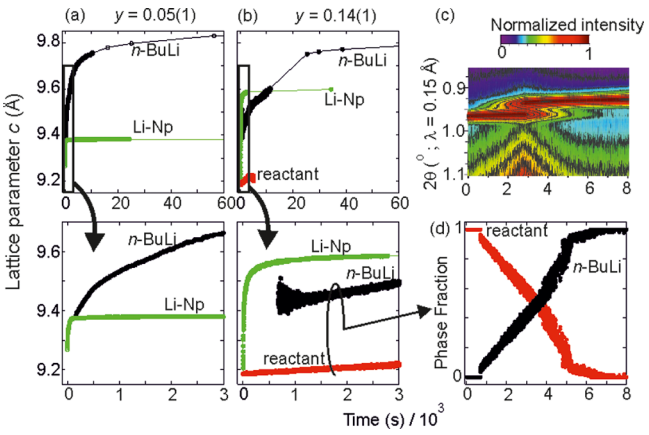

Figure 3. (a, b) Temporal evolution of the c lattice parameter when two samples $Li_{0.8}Fe_{0.2}(OH)Fe_{1-y}Se$ (y = 0.05(1) or 0.14(1); Table S4) were reacted with Li−Np (green) or 0.15 molar *n*-BuLi (black). The lower plots in each case are expansions of the short time regions. (c) The temporal evolution of the 001 reflections measured on I12 for the y = 0.14 sample reacting with *n*-BuLi and (d) shows the temporal evolution of the phase fractions during the early part of that reaction. See Figures S11−S21 and the description of the contrasts in the text.

there is, within the resolution of the data, a continuous transformation in both samples to a single lithiated phase according to eq 1, and these products have different compositions and hence different lattice parameters (Figures 3a,b and S11−S14).

In contrast, with 0.15 molar *n*-BuLi (Figures S15−S17), clear differences in the reactivity are apparent. For the early stages of the reaction with y = 0.14, two phases were resolved: a phase corresponding to the reactant ($c \approx 9.20$ Å) was consumed and replaced by the lithiated phase ($c > 9.4$ Å; Figures 3b−d and S15) over ∼100 min, with no measurable loss of crystalline material during the reaction (Figure 3d). This reaction was significantly slower than with Li−Np. While the reactant phase was being consumed, the lattice parameters of the lithiated product evolved continuously from 9.45 to over 9.5 Å (Figure 3b), and after the complete consumption of the reactant phase the evolution of the lattice parameters of the lithiated phase continued (Figure 3b); the c lattice parameter eventually exceeded that for the product with Li−Np after 3.5 h and continued to increase. Both reactions with *n*-BuLi were stirred continuously and re-examined on the diffractometer every few hours. After 30 h the c lattice parameters in both reactions had increased to similar values of ∼9.8 Å, consistent with the further lithiation described by eq 2, resulting in compositions close to Li(OH)FeSe irrespective of the $Li_{1-x}Fe_x(OH)Fe_{1-y}Se$ reactant composition.

Synthesis and Characterization of Compositions Approaching Li(OH)FeSe. Similar concentrations of *n*-BuLi were reacted ex situ with hydrothermally synthesized samples $Li_{1-x}Fe_x(OH)Fe_{1-y}Se$ with $x \approx 0.2$ and $y \approx 0.1$ (Figures S22−S29; Tables S5 and S6) to probe the formation of compositions approaching Li(OH)FeSe. Two reactions with 0.5 mol equiv of *n*-BuLi at a concentration of 0.23 mol dm^{-3} for 2 d at room temperature yielded products with lattice parameters (a = 3.74 Å and c = 9.76 Å) similar to those of the fully lithiated products of the in situ reactions. The refined compositions from ambient temperature refinements against PND (Figure 4b) and

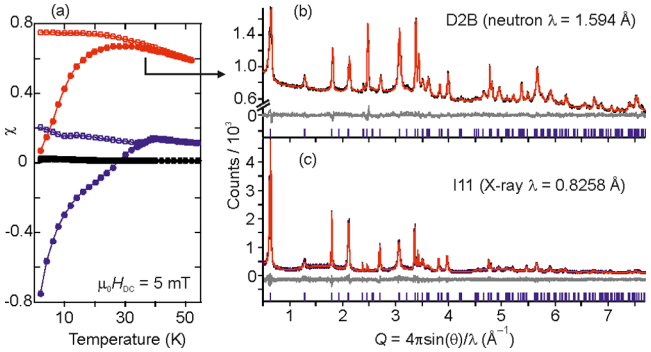

Figure 4. (a) Partial lithiation of a hydrothermally synthesized sample (black) using *n*-BuLi turns on superconductivity (blue) and then turns it off again (red) as the composition Li(OH)FeSe is reached with the expulsion of elemental Fe; zero-field cooled (●) and field-cooled (○) data are shown; (b) PND data and (c) PXRD data of the highly lithiated sample in (a) of refined composition $Li_{0.98(2)}Fe_{0.02(2)}(OH)Fe_{1.00(1)}Li_{0.00(1)}Se$ (Table S5).

synchrotron PXRD (Figure 4c) data produced compositions very close to Li(OH)FeSe (Tables S5 and S6). In the refinements it was assumed that under strongly lithiating conditions the two metal ion sites in the structure would be fully occupied by Fe or Li, and the refined compositions of the two samples were $Li_{0.98(2)}Fe_{0.02(2)}(OH)Fe_{1.00(1)}Li_{0.00(1)}Se$ (Table S5) and $Li_{1.00(2)}Fe_{0.00(2)}(OH)Fe_{0.98(2)}Li_{0.02(2)}Se$ (Table S6). The products were strongly magnetic due to the expelled elemental Fe. The amount of Fe in the bulk samples estimated from magnetization measurements was in line with that suggested by eq 2 and the refined composition of the product. Small differences in the lattice parameters of these compositions close to Li(OH)FeSe, which are obtained in both the in situ and ex situ reactions, suggest that incomplete lithiation of the hydroxide layer or further lithiation to expel further Fe from the selenide layer may occur. These products, which have the composition Li(OH)FeSe within the uncertainty of the refinements, showed no evidence for a superconducting transition (Figure 4a). According to eq 2, the insertion of Li and the reduction of Fe^{2+} with subsequent expulsion as elemental Fe (i.e., $z > 0$) is reductive overall but results in oxidation of the selenide hydroxide phase to a composition close to Li(OH)FeSe. This shows that full occupancy of the Fe sites in the FeSe layer is insufficient to support superconductivity: reduction of Fe below the +2 oxidation state is also required. A PND measurement at 5 K (Figure S29) on the sample of refined composition $Li_{1.00(2)}Fe_{0.00(2)}(OH)Fe_{0.98(2)}Li_{0.02(2)}Se$ revealed no additional scattering from a magnetically long-range ordered state, although anti-ferromagnetic ordering has been proposed for the composition Li(OH)FeSe.[11] Reaction of the hydrothermally synthesized

DOI: 10.1021/acs.inorgchem.6b01734
Inorg. Chem. 2016, 55, 9886−9891

precursor with 0.5 mol equiv of more dilute *n*-BuLi (0.08 mol dm^{-3}) for 6 h at room temperature yielded a product that had not been lithiated as far as the Li(OH)FeSe point and consisted of approximately equal amounts of two phases. It showed evidence for superconductivity as well as enhanced magnetic susceptibility arising from the expulsion of elemental Fe (Figure 4a and Table S5), demonstrating that the superconducting state in these compounds is robust enough to coexist with particles of elemental iron in the sample. The *c* lattice parameters of 9.56 and 9.72 Å for the two phases in this product are consistent with the apparent break in the smooth evolution of the *c* lattice parameter observed in the in situ reaction shown in Figure 3b. This suggests that the lithiation reaction to expel elemental iron, which occurs with *n*-BuLi (eq 2), proceeds via a region where there are two hydroxide selenide phases present.

In situ probing of the lithiation with a large excess of a more concentrated *n*-BuLi solution (1.6 mol dm^{-3}, see Supporting Information) suggested lithiation beyond the Li(OH)FeSe composition, likely via extrusion of Fe from the selenide layer. However, severe loss of crystallinity hampered the analysis of the chemical and structural changes in this process.

Magnetic Properties of Iron in the Hydroxide Layer. Hydrothermally synthesized samples of $Li_{1-x}Fe_x(OH)Fe_{1-y}Se$ often lie outside the superconducting range because they are deficient in Fe in the selenide layer.[10] They show a magnetic transition at ~12 K in the DC magnetic susceptibility, and this is similar for non-superconducting $Li_{1-x}Fe_x(OH)Fe_{1-y}Se$ samples with $x \approx 0.2$ and $0.96 \geq y \geq 0.80$ synthesized from FeSe or from elemental Fe and Se (Figure 5a) and appears in some of the hydrothermally synthesized superconducting samples,[10,12] although not all.[9] We have never observed this magnetic feature in compounds obtained by postsynthetic lithiation where $x < 0.2$ as a result of displacement of Fe from the hydroxide layer into the selenide layer. Magnetization isotherms measured on hydrothermally synthesized samples at 2 K (Figure 5b) show no saturation at applied fields of up to 5 T suggesting the feature observed in the susceptibility measurements at ~12 K may not be a signature of long-range ferromagnetic order. The maximum value of the magnetization at 5 K in a 5 T field was 0.8 μ_B per formula unit, which is consistent with the amount of Fe in the hydroxide layer, although there is variation between samples.

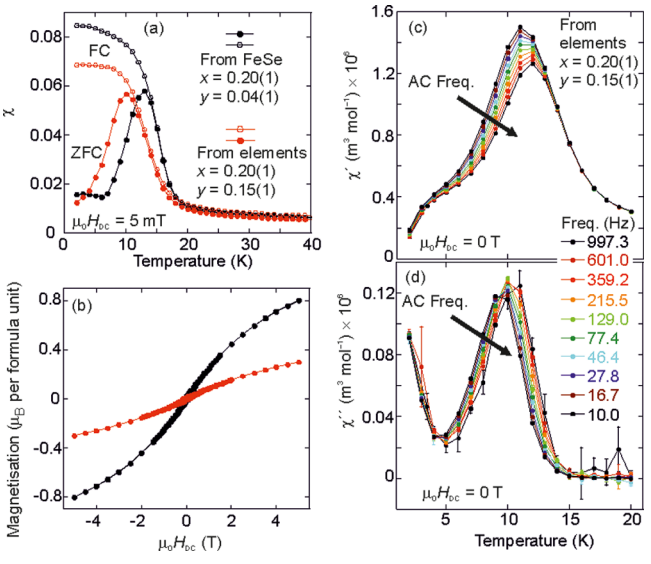

Figure 5. (a) Magnetic susceptibility measurements (DC) between 2 and 40 K for samples of $Li_{1-x}Fe_x(OH)Fe_{1-y}Se$ synthesized from preformed tetragonal FeSe (black) or elemental Fe and Se (red) with ZFC (filled symbols) and FC (empty symbols) measurements shown. (b) Magnetisation isotherms measured (DC) at 2 K on the same samples as in (a). (c) Real (χ') and (d) imaginary (χ'') parts of the AC susceptibility in zero-applied DC field for the sample synthesized from elemental reagents showing the frequency dependence of the magnetism.

PND data collected at 5, 30, and 50 K (see Supporting Information) on samples $Li_{0.79(1)}Fe_{0.21(1)}(OH)Fe_{0.96(1)}Se$ and $Li_{0.79(1)}Fe_{0.21(1)}(OH)Fe_{0.93(1)}Se$ revealed that any enhancement in the intensity of the low-angle Bragg peaks in the 5 K data set due to $k = (0, 0, 0)$ ordering (ferromagnetism) was within the noise level of the data (Figures S5–S8); the refined ordered moment carried by the ions in the hydroxide layer refined to zero within the uncertainty: 0.04(11) μ_B per ion. No additional Bragg peaks were visible, ruling out long-range antiferromagnetic order in line with a recent report of Zhou et al. on the deuterated analogue[17] and a Mössbauer spectroscopy study.[18] Lynn et al.[19] concluded that there was no evidence for long-range ferromagnetic order that would contribute to Bragg peaks, but small-angle neutron scattering measurements showed an onset of magnetic scattering below 12 K, which might be characteristic of an inhomogeneous ferromagnet. Computational investigations of $Li_{0.8}Fe_{0.2}(OH)FeSe$ using a Li/Fe ordered superstructure in the hydroxide layer suggest that the interactions should be ferromagnetic.[20] Claims of antiferromagnetic order below 120 K[21] seem to be a consequence of impure samples.[17]

AC susceptometry was used to characterize the low-temperature magnetic state. In zero applied DC field there is a clear dependence on the AC frequency of the real (χ'; Figure 5c) and imaginary (χ''; Figure 5d) parts of the susceptibility below 14 K, suggesting dynamic effects; the χ' shoulder and χ'' increase at ~4 K indicate additional effects. These features, together with the absence of measurable low-temperature magnetic Bragg scattering, show that the system does not display long-range order of the Fe moments in the dilute lithium iron hydroxide layers. Nor is the behavior consistent with the paramagnetism of noninteracting Fe^{2+} moments in the hydroxide layers, which may only show slow magnetic relaxation in the presence of a DC field exceeding tens of millitesla.[22] The magnetometry is consistent with spin-glass behavior arising from ferromagnetic coupling within clusters of Fe^{2+} moments that will inevitably occur in disordered $Li_{1-x}Fe_x(OH)$ layers (Figure S30). Furthermore, the value of $\Delta T_f/[T_f \Delta(\ln(\omega))]$ (T_f is the temperature of the χ' peak, and ω is the AC frequency), which is used to characterize slow magnetic relaxation, is 0.016(1), which lies in the range characteristic of spin glasses.[22] The dynamic effects warrant further investigation with further techniques and a greater frequency range to elucidate their exact nature and that of the low-temperature feature.

DISCUSSION AND CONCLUSIONS

We have shown that superconductivity in lithium iron hydroxide selenides requires both full occupancy of the Fe sites in the selenide layers *and* reduction of iron below the +2 oxidation state: the formation of the composition Li(OH)FeSe occurs when the $Li_{1-x}Fe_x(OH)Fe_{1-y}Se$ phases are lithiated with *n*-BuLi, and in situ PXRD and other measurements show that this phase, which might be considered the "parent" phase of

DOI: 10.1021/acs.inorgchem.6b01734
Inorg. Chem. 2016, 55, 9886−9891

these hydroxide selenide materials, does not form readily when Li−Np or Li/NH_3 is used as the lithiating reagent. We presume that this is because decomposition of the Li−Np and Li/NH_3 by the products competes with further lithiation, especially when the reaction proceeds beyond the limit of eq 1, while *n*-BuLi is less readily decomposed, allowing further transformation according to eq 2 with the expulsion of elemental Fe and the formation of Li(OH)FeSe. First-principles calculations[11] have predicted that stoichiometric Li(OH)FeSe should have an anti-ferromagnetic ground state that is suppressed on electron doping (enabling superconductivity to emerge); this is consistent with our observation that this parent phase does not exhibit superconductivity, although no indication of magnetic long-range order was observed in our PND measurement. This transformation may be similar to that reported by Lei et al.[23] using electrochemical lithiation, which led to enhancement of superconductivity followed, on further lithiation, by a transition to a semiconducting state. However, in that case the compositional and structural changes were not quantified due to the small sample size. The formation of bulk Li(OH)FeSe is accompanied by loss of crystallinity, which hampers characterization using single-crystal methods. We have examined the low-temperature magnetic transition in compositions $Li_{1-x}Fe_x(OH)Fe_{1-y}Se$ with $x \approx 0.2$ (i.e., iron-rich hydroxide layers), which are not superconducting, and have shown that this transition is consistent with spin glass behavior arising from ferromagnetic coupling of clusters of Fe^{2+} moments in the disordered $Li_{0.8}Fe_{0.2}(OH)$ layers, and there is no evidence for long-range magnetic order arising from these dilute and disordered moments.

■ ASSOCIATED CONTENT

Supporting Information

The Supporting Information is available free of charge on the ACS Publications website at DOI: 10.1021/acs.inorgchem.6b01734.

Further synthesis and characterization details, safety instructions, analysis of ex situ and in situ powder diffraction data (PDF)

■ AUTHOR INFORMATION

Corresponding Author

*E-mail: simon.clarke@chem.ox.ac.uk.

Notes

The authors declare no competing financial interest.

■ ACKNOWLEDGMENTS

We thank: the EPSRC (EP/1017844/1 & EP/M020517/1) and the Leverhulme Trust RPG-2014-221 for financial support; the Diamond Light Source Ltd for beam time (I11 (EE13284) and I12) and support to J.N.B.; the ILL (D2B) and the ISIS facility (GEM Xpress) for neutron beam time; Dr. A. Baker and Dr. C. Murray for assistance on I11, Dr. S. Michalik and Dr. M. Drakopoulos on I12, Dr. E. Suard on D2B, and Dr. R. Smith at ISIS.

■ REFERENCES

(1) Hsu, F.-C.; Luo, J.-Y.; Yeh, K.-W.; Chen, T.-K.; Huang, T.-W.; Wu, P. M.; Lee, Y.-C.; Huang, Y.-L.; Chu, Y.-Y.; Yan, D.-C.; Wu, M.-K. Superconductivity in the PbO-type structure α-FeSe. *Proc. Natl. Acad. Sci. U. S. A.* **2008**, *105*, 14262−14264.

(2) McQueen, T. M.; Huang, Q.; Ksenofontov, V.; Felser, C.; Xu, Q.; Zandbergen, H.; Hor, Y. S.; Allred, J.; Williams, A. J.; Qu, Q.; Checkelsky, J.; Ong, N. P.; Cava, R. J. Extreme sensitivity of superconductivity to stoichiometry in $Fe_{1+\delta}Se$. *Phys. Rev. B: Condens. Matter Mater. Phys.* **2009**, *79*, 014522.

(3) Guo, J.-G.; Jin, S.-F.; Wang, G.; Wang, S.-C.; Zhu, K.-X.; Zhou, T.-T.; He, M.; Chen, X. L. Superconductivity in the iron selenide $K_xFe_2Se_2$ ($0 \le x \le 1.0$). *Phys. Rev. B: Condens. Matter Mater. Phys.* **2010**, *82*, 180520.

(4) Bacsa, J.; Ganin, A. Y.; Takabayashi, Y.; Christensen, K. E.; Prassides, K.; Rosseinsky, M. J.; Claridge, J. B. Cation vacancy order in the $K_{0.8+x}Fe_{1.6-y}Se_2$ system: Five-fold cell expansion accommodates 20% tetrahedral vacancies. *Chem. Sci.* **2011**, *2*, 1054−1058.

(5) Texier, Y.; Deisenhofer, J.; Tsurkan, V.; Loidl, A.; Inosov, D. S.; Friemel, G.; Bobroff, J. NMR Study in the Iron-Selenide $Rb_{0.74}Fe_{1.6}Se_2$: Determination of the Superconducting Phase as Iron Vacancy-Free $Rb_{0.3}Fe_2Se_2$. *Phys. Rev. Lett.* **2012**, *108*, 237002.

(6) Ying, T. P.; Chen, X. L.; Wang, G.; Jin, S. F.; Zhou, T. T.; Lai, X. F.; Zhang, H.; Wang, W. Y. Observation of superconductivity at 30 ∼ 46 K in $A_xFe_2Se_2$ (A = Li, Na, Ba, Sr, Ca, Yb, and Eu). *Sci. Rep.* **2012**, *2*, 426.

(7) Burrard-Lucas, M.; Free, D. G.; Sedlmaier, S. J.; Wright, J. D.; Cassidy, S. J.; Hara, Y.; Corkett, A. J.; Lancaster, T.; Baker, P. J.; Blundell, S. J.; Clarke, S. J. Enhancement of the superconducting transition temperature of FeSe by intercalation of a molecular spacer layer. *Nat. Mater.* **2012**, *12*, 15−19.

(8) Sedlmaier, S. J.; Cassidy, S. J.; Morris, R.; Drakopoulos, M.; Reinhard, C.; Moorhouse, S. J.; O'Hare, D.; Manuel, P.; Khalyavin, D.; Clarke, S. J. Ammonia-Rich High-Temperature Superconducting Intercalates of Iron Selenide Revealed through Time-Resolved in Situ X-ray and Neutron Diffraction. *J. Am. Chem. Soc.* **2014**, *136*, 630−633.

(9) Lu, X. F.; Wang, N. Z.; Zhang, G. H.; Luo, X. G.; Ma, Z. M.; Lei, B.; Huang, F. Q.; Chen, X. H. Superconductivity in $LiFeO_2Fe_2Se_2$ with anti-PbO-type spacer layers. *Phys. Rev. B: Condens. Matter Mater. Phys.* **2014**, *89*, 020507R.

(10) Sun, H.; Woodruff, D. N.; Cassidy, S. J.; Allcroft, G. M.; Sedlmaier, S. J.; Thompson, A. L.; Bingham, P. A.; Forder, S. D.; Cartenet, S.; Mary, N.; Ramos, S.; Foronda, F. R.; Williams, B. H.; Li, X.; Blundell, S. J.; Clarke, S. J. Soft Chemical Control of Superconductivity in Lithium Iron Selenide Hydroxides $Li_{1-x}Fe_x(OH)Fe_{1-y}Se$. *Inorg. Chem.* **2015**, *54*, 1958−1964.

(11) Wang, G.; Yi, X.; Shi, X. The electronic structure and magnetism of a new layered iron selenide superconductor: LiOHFeSe. *Phys. Lett. A* **2015**, *379*, 2106−2109.

(12) Pachmayr, U.; Nitsche, F.; Luetkens, H.; Kamusella, S.; Brückner, F.; Sarkar, R.; Klauss, H.-H.; Johrendt, D. Coexistence of 3d-ferromagnetism and superconductivity in $[(Li_{1-x}Fe_x)OH](Fe_{1-y}Li_y)Se$. *Angew. Chem., Int. Ed.* **2015**, *54*, 293−297.

(13) Lu, X. F.; Wang, N. Z.; Wu, H.; Wu, Y. P.; Zhao, D.; Zeng, X. Z.; Luo, X. G.; Wu, T.; Bao, W.; Zhang, G. H.; Huang, F. Q.; Huang, Q. Z.; Chen, X. H. Coexistence of superconductivity and antiferromagnetism in $(Li_{0.8}Fe_{0.2})OHFeSe$. *Nat. Mater.* **2014**, *14*, 325−329.

(14) Betteridge, P. W.; Carruthers, J. R.; Cooper, R. I.; Prout, K.; Watkin, D. J. CRYSTALS version 12: software for guided crystal structure analysis. *J. Appl. Crystallogr.* **2003**, *36*, 1487−1487.

(15) Coelho, A. A. *TOPAS Academic,* Version 5; Coelho Software: Brisbane, Australia, 2012.

(16) Blundell, S. J. *Magnetism in Condensed Matter;* Oxford University Press: Oxford, U.K, 2001.

(17) Zhou, X.; Borg, C. K. H.; Lynn, J. W.; Saha, S. R.; Paglione, J.; Rodriguez, E. E. The preparation and phase diagrams of $(^7Li_{1-x}Fe_xOD)FeSe$ and $(Li_{1-x}Fe_xOH)FeSe$ superconductors. *J. Mater. Chem. C* **2016**, *4*, 3934−3941.

(18) Nejadsattari, F.; Stadnik, Z. M. Search for Fe magnetic ordering in the 40 K superconductor $(Li_{0.8}Fe_{0.2})OHFeSe$. *J. Alloys Compd.* **2015**, *652*, 470−478.

DOI: 10.1021/acs.inorgchem.6b01734
Inorg. Chem. 2016, 55, 9886−9891

(19) Lynn, J. W.; Zhou, X.; Borg, C. K. H.; Saha, S. R.; Paglione, J.; Rodriguez, E. E. Neutron investigation of the magnetic scattering in an iron-based ferromagnetic superconductor. *Phys. Rev. B: Condens. Matter Mater. Phys.* **2015**, *92*, 060510R.
(20) Nekrasov, I. A.; Sadovskii, M. V. Electronic and magnetic properties of the new iron-based superconductor $[Li_{1-x}Fe_xOH]FeSe$. *JETP Lett.* **2015**, *101*, 47−50.
(21) Dong, X.; Zhou, H.; Yang, H.; Yuan, J.; Jin, K.; Zhou, F.; Yuan, D.; Wei, L.; Li, J.; Wang, X.; et al. Phase Diagram of $(Li_{1-x}Fe_x)$-OHFeSe: A Bridge between Iron Selenide and Arsenide Superconductors. *J. Am. Chem. Soc.* **2015**, *137*, 66−69.
(22) Gatteschi, D.; Sessoli, R.; Villain, J. *Molecular Nanomagnets;* Oxford University Press: Oxford, U.K, 2011.
(23) Lei, B.; Xiang, Z. J.; Lu, X. F.; Wang, N. Z.; Chang, J. R.; Shang, C.; Luo, X. G.; Wu, T.; Sun, Z.; Chen, X. H.; et al. Gate-tuned superconductor-insulator transition in (Li,Fe)OHFeSe. *Phys. Rev. B: Condens. Matter Mater. Phys.* **2016**, *93*, 060501.

DOI: 10.1021/acs.inorgchem.6b01734
Inorg. Chem. 2016, 55, 9886−9891